Experimental Evaluation of Dynamic Young's Moduli and Anisotropy in Shales.

Andre Panfiloff and Manika Prasad, Colorado School of Mines, Colorado, USA.*

Summary

Dynamic elastic mechanical properties and transverse anisotropy in shales are very important to consider in estimation of the in-situ stress, petrophysical and geophysical analyses. Typically, they are calculated based on the acquired ultrasonic velocities under simulated close to in-situ conditions in a laboratory environment. Specifically, compressional and shear velocities are measured in 0°, 45°, and 90° orientation to bedding plane of the particular shale sample. In previous studies, these measurements were accomplished using three-plug-method, which would require to core three independent core plugs oriented horizontally, in 45°, and vertically. In this study, we designed and implemented a special core holder to perform non-destructive, efficient, reliable, multidirectional, and simultaneous ultrasonic compressional and shear velocity measurements on the single 1.5 in. cylindrical core plug under simulated in-situ conditions.

Our results provide an insight into the elastic mechanical behavior and the degree of anisotropy that organic shales may experience under in-situ conditions. Specifically, we find and quantify that the Young's moduli in the direction parallel to the bedding plane is greater than perpendicular to it. The degree of anisotropy in terms of Thomsen anisotropy parameters and horizontal to vertical ratio of Young's moduli have been estimated under elevated pressures on the up and down pressure cycles. It was observed that anisotropy decreases dramatically with increase in pressure, but does not approach zero. It was concluded that this observed phenomena at high confining pressures may potentially be explained by the existence of some degree of intrinsic anisotropy in organic matter and clay particles.

The estimation of Young's moduli in vertical and horizontal directions has been investigated based on the application of the two different sets of equations. One is the appropriate isotropic equations, and the second is VTI equations. It was discovered that the degree of discrepancy between estimation of Young's moduli by these two methods is on the order of 15%-20%. This result is a very important finding. Thus, it is crucial to obtain an accurate direct measurement of the C_{13} stiffness coefficient in order to have true estimation of the vertical and horizontal Young's moduli.

Introduction

The anisotropic nature of shales creates significant problems in seismic exploration (Thomsen, 1986), specifically, in fluid identification (Sheriff, 2002). Ignoring anisotropy can lead to miscalculation of elastic mechanical parameters and wrong estimates of in-situ stresses (Thomsen, 1986). In order to accurately evaluate dynamic elastic properties and the degree of anisotropy of organic rich shale rock, compressional and shear velocity measurements must be acquired in the lab under simulated in-situ conditions often under an important assumption of a vertical transverse isotropy (VTI) model. In VTI media, rock properties vary depending on direction with respect to axis of symmetry. Typically, the symmetry axis is orthogonal to the bedding plane orientation. In order to fully describe elastic mechanic properties of shales, five independent stiffness coefficients must be calculated based on the acquired compressional and shear velocities in parallel (0°) direction, 45° oblique angle, and normal (90°) to the bedding plane orientation in a shale sample (Vernik and Nur 1992; Hornby 1998; Sondergeld and Rai 2011). Often, reliable laboratory anisotropic velocity measurements with as close to the in-situ conditions as possible are challenging. Typically, the so-called "three-plug-method" is used for analysis: three independent core plugs are cored from a larger conventionally drilled core in the directions orthogonal, horizontal, and at 45° oblique angle to the axis of the core or bedding plane. Disadvantages of the three-plug method are: three separate measurement for three plugs are needed requiring time for core preparation and measurement processes; because of the heterogeneous nature of the organic-rich shale samples, the three different core samples might not represent the same rock. The ultrasonic velocity measurements in on organic-rich shales using a three-plug-method were conducted by Vernik and Nur (1992), Vernik and Liu (1997), Hornby (1998), Sondergeld and Rai (2011). The three-plug method is usually employed and the crucial C_{13} stiffness coefficient is either measured with some unknown degree of error, approximated or simulated. This is due to technical difficulty of measuring compressional and shear velocities at precise 45° oblique angle to bedding under simulated in-situ conditions. However, Prasad and Manghnani (1997), Wang (2002), Dewhurst and Siggins (2006), and Woodruff (2013) have established that ultrasonic multidirectional measurements on a single core at the same pressure can be successfully performed. Similar measurement on a single core plug with transducers attached directly on the surface of the rock were performed by Dewhurst and Siggings (2006) and Wang (2002).

In this study, we analyze velocity and anisotropy measurements on organic-rich shale samples, and quantify anisotropic results for dynamic Young's moduli.

Core Availability and Experimental Setup

Four shale rock sample plugs were 1.5 inches in diameter and had been provided by an oil and gas exploration

company for this study. The names of the plugs are L1, L2, L3, and L4.

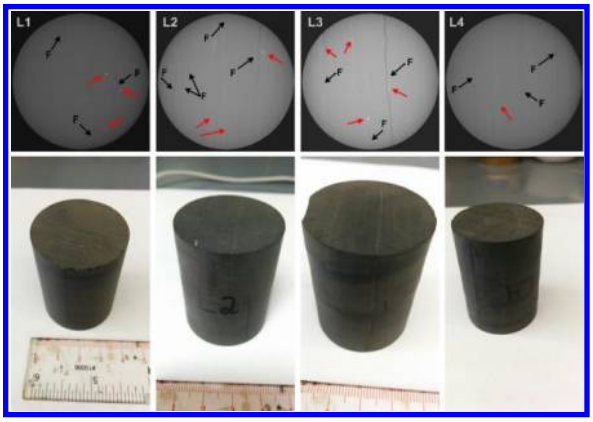

Figure 1: X-ray CT scan images and photo images of the L-set mudrock samples. The main observed feature for all L-set samples is the presence of micro-fractures and their alignment with the bedding plane.

In this study, we designed, built, and used a special core jacket holder (PLP core jacket holder) to carry out multidirectional and simultaneous ultrasonic compressional and shear velocities measurements under hydraulic confining pressure. The jacket was tested and calibrated using standard samples of aluminum and sandstones. It was then used to measure four organic-rich shale core samples.

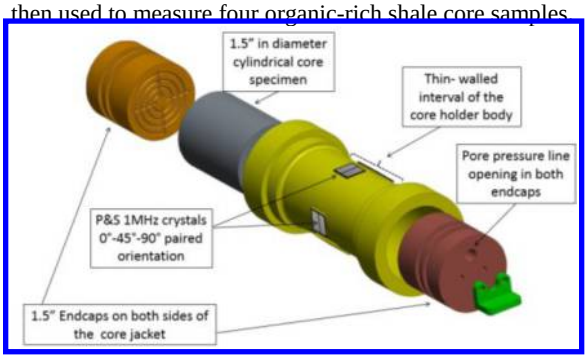

Figure 2: The sketch of the PLP core jacket holder design presented using Solidworks software. The 1.5" core sample (dark grey color) is inserted into the core jacket (yellow color). The core sample is inserted into a flexible plastic sleeve. Compressional and shear piezoelectric transducers (1 MHz P and S crystals) are glued onto the outside surface of the flat areas of the sleeve. A plastic-glass compound type of material was used in the fabrication of endcaps and proved to be a success in providing necessary integrity to withstand high confining pressures. Patent Application Number: US 62/304,479.

Methods

Based on the acquired velocity measurements, the full elastic tensor for VTI medium was defined, and dynamic Young's moduli and degree of anisotropy were estimated.

Young's moduli parallel to bedding, $E_{horizontal}$ and perpendicular to bedding, $E_{vertical}$, are calculated using the following formulas (King 1964):

$$E_{vertical\ (TRUE)} = E_3 = \frac{D}{C_{11}^{\ 2} - C_{12}^{\ 2}}$$

$$E_{horizontal\ (TRUE)} = E_1 = \frac{D}{C_{11}C_{33} - C_{13}^{\ 2}}$$

In the Equations 1 and 2 D is a determinant, which is defined as following:

$$\begin{vmatrix} C_{11} & C_{12} & C_{13} \\ C_{12} & C_{11} & C_{13} \\ C_{13} & C_{13} & C_{33} \end{vmatrix}$$

The dynamic Young's moduli in vertical and horizontal directions for the VTI medium are estimated using the Equations 1 and 2. However, very often Young's moduli in these two directions cannot be calculated because of the technical difficulty of measuring the C_{13} stiffness coefficient (Wang 2002; Sondergeld and Rai 2011). In that case the isotropic equations are used to estimate apparent Young's moduli (Sone and Zoback 2013). These isotropic equations require four independent coefficients calculated from compressional and shear velocities in vertical and horizontal direction to the bedding plane (Thomsen 2013).

$$E_{horizontal\ (APPARENT)} = \frac{C_{66}(3C_{11} - 4C_{66})}{C_{11} - C_{66}}$$

$$E_{vertical\ (APPARENT)} = \frac{C_{44}(3C_{33} - 4C_{44})}{C_{33} - C_{44}}$$

XRD Mineralogy, Geochemical, WIP, and Pore Size Distribution Results

The XRD mineralogy for L-set shale core samples is the following. The clay content varies from 19% to 42%; the carbonate content varies between 32% and 49%, quartz content is 23% on average, and pyrite content is 3% to 4% by weight.

Based on the results of SRA and LECO TOC data results, the L-set shale samples belong to the interval of oil window, and indicative of kerogen type II and type III. This is supported by values of Tmax, which fall into interval between 435°C and 450°C. The TOC content is 4.4%, 5.4%, 5.5%, and 5.9% for core samples L1, L2, L3, and L4 respectively.

Nitrogen adsorption results are presented in terms of specific surface area (SSA) of the specimen in m^2/g, pore

volume based on BJH theory inversion in cm^2/g, estimated average pore throat size based on pore size distribution data in nm. The L-set clearly shows a unimodal distribution and depicts significant peaks at 20-100 nm for all L-set samples, except the L2 sample. The PSD for the L-2 sample indicates a presence of pores greater than 200 nm, which is the detection ceiling of the nitrogen adsorption ASAP 2020 instrument (Figure 3). It is important to note that the L2 sample has the highest clay content.

Lastly, the porosity is appraised by bulk volume per unit mass obtained from the WIP results.

Lastly, the porosity is appraised by bulk volume per unit mass obtained from the WIP results. The average bulk density for L-set is 2.35 g/cc. The average grain densities for L-set is 2.435 g/cc respectively. The L-set has the porosity of 6.15% on average.

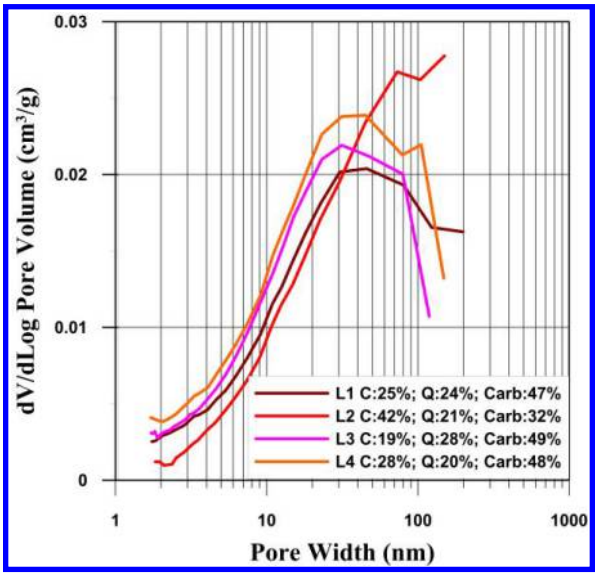

Figure 3: The Pore size distribution of the L-set samples using nitrogen adsorption method. The appropriate mineralogy data for appropriate L-set shale samples is indicated in the bottom right corner.

Ultrasonic Velocity Results

We obtained results and observed effects of the ultrasonic compressional and shear velocities in three essential directions as a function of confining pressure. The three prime directions in this experiment are the following: horizontal, oblique 45 degree angle, and vertical, which are 0°, 45°, and 90° respective to the bedding plane and the primary micro- and stress induced fractures' orientation direction of the mudrock samples.

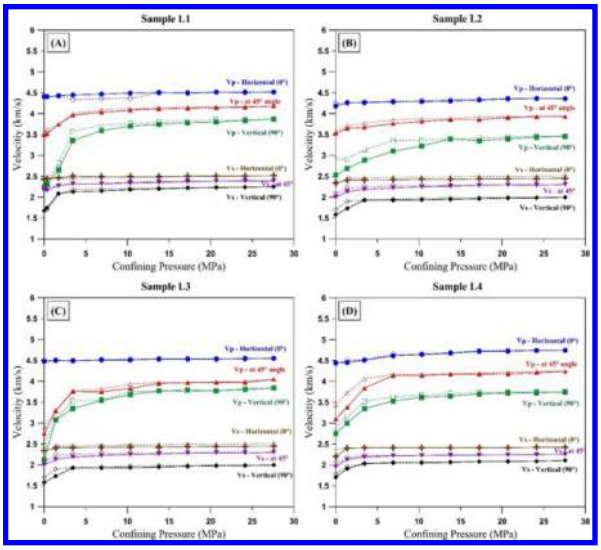

Figure 4: Compressional and shear velocities as a function of confining pressure and direction. (A) Crossplot of results for sample L1. (B) Crossplot of results for sample L2. (C) L3 data crossplot. (D) Crossplot of results for sample L4.

VTI Dynamic Young's Moduli and Degree of Anisotropy as a Function of Confining Pressure

Young's moduli in vertical and horizontal direction estimated for VTI symmetry show that both moduli increase with applied confining pressure. There is a greater increase of Young's moduli in vertical direction from its initial condition as compared to the increase in Young's modulus in the horizontal direction for all shale samples.

The stiffening of the elastic moduli is observed at higher pressures, and possibly extends beyond the maximum tested pressure of 27.6 MPa, suggesting some pore and microfracture compliance at higher pressures (Figure 5).

Anisotropy is presented in terms of Thomsen parameters and the horizontal to vertical Young's moduli ratio, Eh/Ev calculated from the elastic stiffness coefficients for VTI medium and analyzed as functions of confining pressure. Figures 6 shows that the Thomsen anisotropy parameters L-set are generally decreased as confining pressure increased. This decrease in anisotropy suggest presence of two types of anisotropy: microfractures and compliant pores that close with pressure, and intrinsic type of anisotropy that is independent of pressures. Furthermore, some degree of hysteresis is observed and can be explained by some degree of the mechanical deformation and irreversible closure of microfractures with increasing pressure.

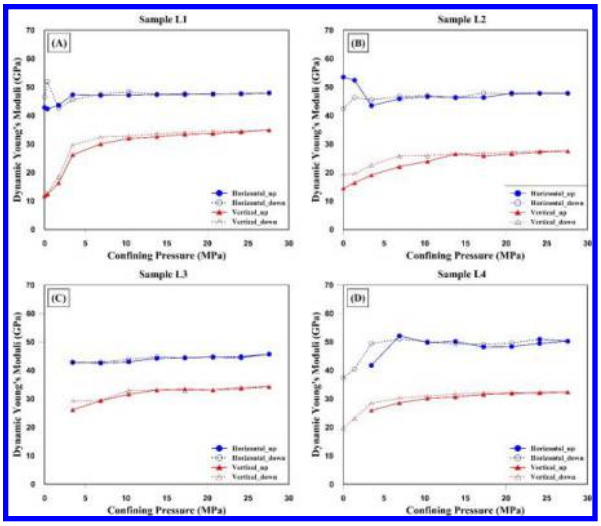

Figure 5: Estimated true dynamic Young's moduli in vertical and horizontal directions. The difference between Young's moduli in these two direction is greater for the sample L4 (D), and the sample L2 (B).

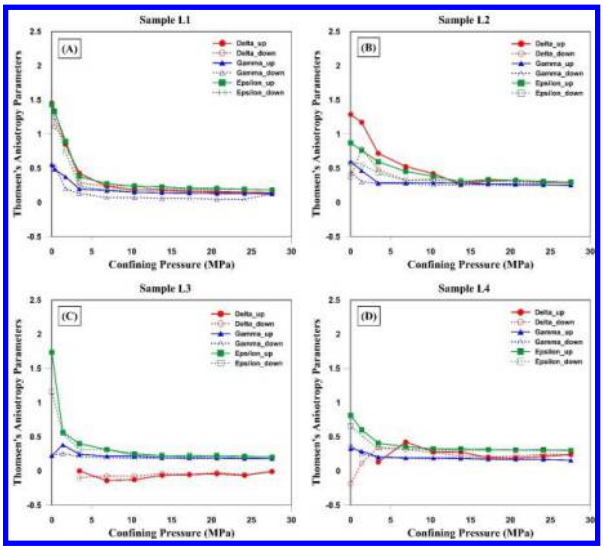

Figure 6: The degree of anisotropy in terms of Thomsen anisotropy parameters as a function of confining pressure for L-set shale samples on the up and down confining pressure cycles.

The degree of anisotropy in shales is can also be expressed by the ratio of Young's moduli in horizontal and vertical directions as functions of confining pressure (Figure 4.18). This is a convenient way to compare the degree of anisotropy in shales at benchtop and under simulated in-situ conditions. As for the Thomsen's parameters, E_h/E_v also show that microfractures and compliant pores close at high pressure, but there is still high degree of anisotropy which most likely credited to the intrinsic anisotropy of shales.

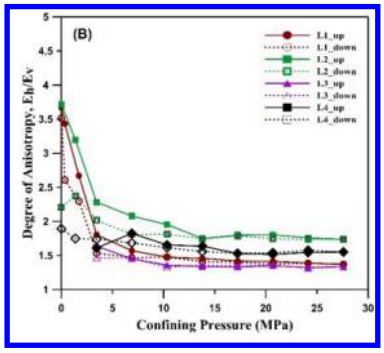

Figure 7: Degree of anisotropy in terms of E_h/E_v as a function of confining pressure on the up and down cycle for L-set shale samples.

Discrepancy between the True and Apparent Estimation of Young's Moduli

A comparison between true and apparent dynamic Young's moduli in vertical and horizontal directions for 11 shale samples at maximum tested pressure of 27.6 MPa showed that the true dynamic Young's moduli is greater on the order of 15% on average in comparison to the apparent dynamic Young's moduli in appropriate directions. By ignoring this effect, the Eh and Ev stress contrast can be either underestimated or overestimated leading to false assessment of failure potential in a rock formation.

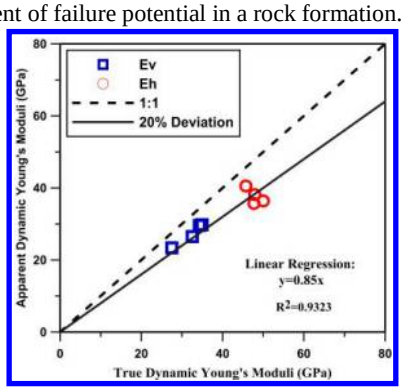

Conclusions

The newly designed core holder reduces sample preparation time from 20 days to under one hour. The samples are recovered at the end of the pressure measurement, and measurements are repeatable. Young's moduli in the bedding parallel direction are about 1.5 to 2 times greater than in the bedding perpendicular direction. Using isotropic equations for each direction underestimates Young's moduli by 15%-20% as compared to calculations using true VTI equations leading to wrong failure potential estimates. Anisotropy in shales is related to presence of cracks that close at pressure conditions as well as existence of layers and laminations.

EDITED REFERENCES

Note: This reference list is a copyedited version of the reference list submitted by the author. Reference lists for the 2016 SEG Technical Program Expanded Abstracts have been copyedited so that references provided with the online metadata for each paper will achieve a high degree of linking to cited sources that appear on the Web.

REFERENCES

Dewhurst, D. N., and A. F. Siggins, 2006, Impact of fabric, microcracks and stress field on shale anisotropy: Geophysical Journal International, **165**, 135–148, http://dx.doi.org/10.1111/j.1365-246X.2006.02834.x.

Hornby, B. E., 1998, Experimental laboratory determination of the dynamic elastic properties of wet, Drained Shales: Journal of Geophysical research: Solid Earth, **103**, 29,945–29,964, http://dx.doi.org/10.1029/97JB02380.

Prasad, M., and M. H. Manghnani, 1997, Effects of pore and differential pressure on compressional wave velocity and quality factor in berea and michigan sandstones: Geophysics, **62**, 1163–1176, http://dx.doi.org/10.1190/1.1444217.

Sone, H., and M. D. Zoback, 2013, Mechanical properties of shale-gas reservoir rocks—Part 1: Static and dynamic elastic properties and anisotropy: Geophysics, **78**, no. 5, D381–D392, http://dx.doi.org/10.1190/GEO2013-0050.1.

Sondergeld, C. H. and C. S. Rai, 2011, Elastic anisotropy of shales: The Leading Edge, **30**, 324–331, http://dx.doi.org/10.1190/1.3567264.

Thomsen, L., 1986, Weak elastic anisotropy: Geophysics, **51,** 1954–1966, http://dx.doi.org/10.1190/1.1442051.

Vernik, L., and X. Liu, 1997, Velocity anisotropy in shales: A petrophysical study: Geophysics, **2**, 521–532, http://dx.doi.org/10.1190/1.1444162.

Vernik, L., and A. Nur, 1992, Ultrasonic velocity and anisotropy of hydrocarbon source rocks: Geophysics, **57**, 727–735, http://dx.doi.org/10.1190/1.1443286.

Wang, Z, 2002, Seismic anisotropy in sedimentary rocks, Part 2: Laboratory Data: Geophysics, **67**, 1423–1440, http://dx.doi.org/10.1190/1.1512743.

Woodruff, W. F., 2013, Multiscale properties of unconventional reservoir rocks: Ph.D. thesis, Colorado School of Mines.